

## **Preparation of efficient quercetin delivery system on Zn-modified mesoporous**

### **SBA-15 silica carrier**

Ivalina Trendafilova<sup>1</sup>, Agnes Szegedi<sup>2</sup>, Judith Mihály<sup>2</sup>, Georgi Momekov<sup>3</sup>, Nadejda Lihareva<sup>4</sup>, Margarita Popova<sup>1\*</sup>

<sup>1</sup>Institute of Organic Chemistry with Centre of Phytochemistry, Bulgarian Academy of Sciences, 1113 Sofia, Bulgaria

(\*e-mail: [mpopova@orgchm.bas.bg](mailto:mpopova@orgchm.bas.bg), tel: +359 879 85 70 79, fax: + 359 2 8700 225)

<sup>2</sup>Research Centre for Natural Sciences, Institute of Materials and Environmental Chemistry, Hungarian Academy of Sciences, 1117 Budapest, Magyar tudósok krt. 2., Hungary

<sup>3</sup> Faculty of Pharmacy, Medical University of Sofia, 1000 Sofia, Bulgaria

<sup>4</sup> Institute of Mineralogy and Crystallography, Bulgarian Academy of Sciences, Sofia, Bulgaria

### ***Abstract***

Mesoporous silica material type SBA-15 was modified with different amounts of Zn (2 and 4 wt. %) by incipient wetness impregnation method in ethanol. The parent, Zn-modified and quercetin loaded samples, were characterized by XRD, N<sub>2</sub> physisorption, TEM, thermal gravimetric analysis, UV-Vis and FT-IR spectroscopies and *in vitro* release of quercetin at pH 5.5 which is typical of dermal formulations. By this loading method anhydrous quercetin was formed on the silica carrier. It was found that the different hydrate forms of quercetin (dihydrate, monohydrate, anhydrite) significantly influence the physico-chemical properties of the delivery system. It was found that hydrate forms of quercetin can be differentiated by XRD and by FT-IR spectroscopic methods. Thus, by evaluating the interaction of the drug with the silica carrier the changes due to its hydration state always have to be taken into account. Formation of Zn-quercetin complex was evidenced on zinc modified SBA-15 silica

by FT-IR spectroscopy. High quercetin loading capacity (over 40 wt. %) could be achieved on the parent and Zn-containing SBA-15 samples. The *in-vitro* release process at pH=5.5 showed slower quercetin release from Zn-modified SBA-15 samples compared to the parent one. Additionally, the comparative cytotoxic experiments evidenced that quercetin encapsulated in Zn-modified silica carriers has superior antineoplastic potential against HUT-29 cells compared to free drug. Zn-modified SBA-15 silica particles could be promising carriers for dermal delivery of quercetin.

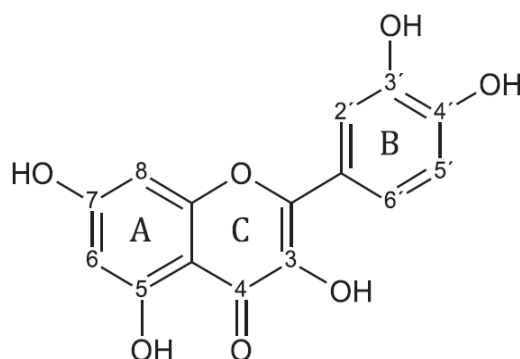
**Key words:** quercetin hydrates, quercetin loading, *in vitro* release, SBA-15, dermal application, cytotoxicity

## ***Introduction***

The tremendous interest in the recent years towards elaboration of mesoporous silica materials as potential carriers for drugs is based on the advantages of these materials, such as biocompatibility, high specific surface and pore volume, tunable pore size, controlled particle size and morphology and possibility for surface functionalization [1-7]. In the preparation of mesoporous silica nanoparticulate systems a feasible approach is to circumvent the problems associated with poor aqueous solubility, low bioavailability and chemical stability of the loaded substance. SBA-15 is one of the most common types of mesoporous nanoparticle, and its large, hexagonally arrayed pores are capable of ensuring the access of large drug molecules. The appropriate surface modification of the silica matrix with metal ions can optimize the loading efficacy and the release kinetic of the drug [1,4,5].

In the recent years natural flavonoids have attracted research interest due to their pleiotropic therapeutic potential. Quercetin (2-(3,4-dihydroxyphenyl)-3,5,7-trihydroxy-4H-chromen-4-one) is one of the most common flavonols present in nature, a strong antioxidant and a major

dietary flavonoid. The primary dietary sources of quercetin include onions, apples, wine, berries and tea [8-11].



**Scheme 1** Molecular structure of quercetin

It has been extensively studied because of its broad-spectrum pharmacological activities. Quercetin is known to exhibit anticancer, antiviral, antimutagenic and lipid peroxidation inhibitory effects. Initially these effects have been attributed to the strong antioxidant properties of quercetin, because of its ability to scavenge free radicals and the influence on the intracellular redox status. The antioxidant action appears to be a combination of reaction with free radicals, inhibition of xanthine oxidation and lipid peroxidation [12-14] and metal ion complexation [15]. A vast number of data have unambiguously shown that quercetin is endowed by prominent anticancer activity, mediated by pleiotropic actions on malignant cell signaling pathways. It was found that quercetin can regulate cell cycle by modulating several molecular targets, including p21, cyclin B, p27, and topoisomerase [16]. In addition, quercetin displays specific inhibitory effects in various groups of kinases, including Janus kinases (JAK) and especially JAK-3 kinase, which is a non-receptor tyrosine kinase predominantly expressed in hematopoietic cells [17]. Abnormal activation of JAK-kinase is attributed to human hematological malignancies including the orphan-disease cutaneous T-cell lymphoma (CTCL) [18].

Unfortunately, the clinical realization of quercetin's therapeutic potential is greatly hampered due to unfavorable physicochemical and pharmacokinetic properties. Quercetin is characterized with very low aqueous solubility and chemical instability, which respond in low bioavailability. To overcome these unfavorable characteristics of the drug a possible approach is the elaboration of carriers for optimized oral, systemic, site-specific or topical delivery of quercetin. Quercetin has been formulated in liposomes [19], nanoparticles [20,21], metal ions complexes [15]. Being a strong antioxidant quercetin acts mainly by chelating metal ions ( $\text{Fe}^{2+}$ ,  $\text{Fe}^{3+}$ ,  $\text{Cu}^{2+}$ )[8]. On the other hand Zn as a chelating agent can form complexes with large numbers of biological active molecules like peptides [22], flavonoids, DNA [23], etc. On this ground a novel approach to optimized delivery of quercetin or its analogs is based on encapsulation in Zn-modified mesoporous silica material. Moreover, modification with Zn is suitable for elaboration of carriers for dermal drug delivery because it is the most abundant essential transition element in organisms after Fe and it has proven antibacterial activity. Therefore, numerous studies have been devoted to the mechanism of metal ion complexation of quercetin, the structure and stability of the formed complexes as well as the effect of solvent and media [23-25]. Accordingly, we focus our attention on the development of dual-component formulations with Zn oxide species and quercetin supported on mesoporous silica SBA-15 carrier.

In the present study the formation of the complexes between quercetin and the silanol groups of the parent or Zn modified SBA-15 mesoporous silica was investigated. *In vitro* release profiles of quercetin from the obtained mesoporous silica particles were studied in respect of their possible application as dermal formulations against cutaneous T-cell lymphoma. The cytotoxic potential of non-loaded and quercetin loaded particles was investigated against two types of human cells, including HUT-29 cells as a model of CTCL *in vitro*.

## ***2. Materials and methods***

### ***2.1. Materials***

PEO<sub>20</sub>PPO<sub>70</sub>PEO<sub>20</sub> (Pluronic P123) was purchased from BASF. Quercetin (>99.5 %), and tetraethyl orthosilicate (TEOS) was provided by Aldrich.

### ***2.2. Synthesis of SBA-15 silica material***

SBA-15 silica was prepared following the method described by Zhao et al. [26]. In brief, 2 g of P123 was dissolved in a solution of 60 ml deionized water and 6,18 ml HCl (2M) at 35°C, followed by addition of 4 g TEOS. The mixture was stirred at 35°C for 24 h before autoclaving in a Teflon bottle at 95°C for 24 h. The solid product was filtered and washed three times with deionized water. Calcination for template removal was conducted in air with a heating rate of 1°C/min at 550°C for 6 h.

### ***2.3. Functionalization of SBA-15 by Zn***

An incipient wetness impregnation technique with Zn(CH<sub>3</sub>COO)<sub>2</sub>·2H<sub>2</sub>O was applied for loading of 2 or 4 wt. % zinc oxide. In a typical experiment zinc acetate - 20.14 mg or 40.28 mg for 2 or 4 wt. % zinc, respectively, was dissolved in 1 ml ethanol (99.9%) and 300 mg of mesoporous support SBA-15 was added. The functionalization was performed at room temperature. Samples were calcined in air at 500°C for 3 hours and designated as SBA-15x where x= 2 or 4 wt.% Zn.

### ***2.4. Quercetin loading***

SBA-15 and quercetin in ratio 1:1 were stirred in 1 ml ethanol till the total evaporation of the solvent. Then the powdered products were washed 3 times with 5 ml water, and dried at 40°C

overnight. The quercetin loaded SBA-15 formulation was designated as SBA-15Qu, SBA-15ZnxQu, where  $x=2$  and 4 wt.%.

As reference materials for XRD and FT-IR investigations quercetin dihydrate and anhydrite were prepared. Quercetin dihydrate was prepared by recrystallizing the parent quercetin material in ethanol than keeping it in controlled humidity atmosphere. Quercetin anhydrite was prepared by recrystallizing it in methanol several times than heat treated at 120°C for 2h. Hydration state of the reference materials was checked by XRD and by thermogravimetric analysis. The FT-IR spectrum of the prepared quercetin dihydrate is identical with that of found in Aldrich library of FT-IR spectra.

## **2.5. Characterization**

X-ray powder diffraction patterns were recorded by a Philips PW 1810/3710 diffractometer with Bragg-Brentano parafocusing geometry applying monochromatized  $\text{CuK}\alpha$  ( $\lambda=0.15418$  nm) radiation (40 kV, 35 mA) and a proportional counter. In situ high temperature XRPD measurements were carried out in an HTK-1200 Anton-Paar chamber in air with temperature programming. Simulated patterns of quercetin dihydrate and monohydrate were calculated based on single crystal data of Cambridge structural database by Mercury 3.8 software (dihydrate-Fefbex01, monohydrate- Akijek01), whereas that of quercetin anhydrite was based on data of Filip et. al. (Quer3), determined by NMR and powder diffraction measurements [27].

Nitrogen physisorption measurements were carried out at -196°C using Thermo Scientific Surfer automatic volumetric adsorption analyzer. Before the analysis, silica samples were outgassed under high vacuum for 2 h at 250°C, whereas drug loaded samples were pretreated at 80°C for 3 h [28,29]. The pore-size distributions were calculated from the desorption isotherms by the BJH method.

Diffuse reflectance UV-Vis spectra were measured at ambient by Jasco V-670 UV-Vis spectrophotometer equipped with an NV-470 type integrating sphere using BaSO<sub>4</sub> reflectance standard as reference.

TEM images were taken using a MORGAGNI 268D TEM (100 kV; W filament; point-resolution = 0.5 nm). Samples were suspended in a small amount of ethanol and a drop of suspension was deposited onto the copper grid covered by carbon supporting film and dried at ambient.

Thermogravimetric measurements were performed with a Setaram TG92 instrument with a heating rate of 5°C/min in air flow.

Attenuated Total Reflection Infrared (ATR-FT-IR) spectra were recorded by means of a Varian Scimitar 2000 FT-IR spectrometer equipped with a MCT (mercury-cadmium-tellur) detector and a single reflection ATR unit (SPECAC “Golden Gate”) with diamond ATR element. In general, 128 scans and 4 cm<sup>-1</sup> resolution was applied. For all spectra ATR-correction was performed (Varian ResPro 4.0 software).

## ***2.6. In-vitro release study***

In-vitro quercetin release study was performed in buffer (pH = 5.5) at 37°C. The drug-loaded particles (2 mg) were incubated in 200 ml phosphate buffer with pH=5.5 at 37°C under stirring (300 rpm). At appropriate time intervals, 3 ml samples were withdrawn from the release medium and analyzed by UV-Vis spectroscopy at a wavelength of 367 nm. The concentration of the released quercetin was calculated according to the calibration curves prepared in pH=5.5 solution ( $r > 0.9993$ ).

## ***2.7. Cell lines and culture conditions***

The cell lines HEK-293 (human embryonal kidney cells) and HUT-78 (cutaneous T-cell lymphoma - CTCL) were supplied by DSMZ GmbH, Germany. Cells were cultured routinely in a controlled environment: 37°C in 5% CO<sub>2</sub> humidified atmosphere. All cell lines were maintained in RPMI 1640 supplemented with 2 mM L-glutamine and 10% fetal calf serum. The cell lines were subcultured biweekly to maintain continuous logarithmic growth.

## ***2.8. Cytotoxicity assay***

Cell survival was evaluated by using the standard MTT-dye reduction assay [30] with slight modifications [31]. The method is based on the ability of viable cells to metabolize a yellow tetrazolium salt to a violet formazan product which is detected spectrophotometrically at 527 nm. Exponentially growing cells were plated in 96-well sterile plates at a density of 10<sup>4</sup> cells/well in 100 µL of medium and were incubated for 24 h. Then quercetin and the tested mesoporous silica particles were applied for 72 h, using for each concentration a set of 8 wells. After a 72-h continuous exposure period, 10 µL aliquots from a 5 mg/ml MTT solution were added to each well and the plates were further incubated for 4 h at 37°C in a humidified 5 % CO<sub>2</sub> atmosphere. The formazan crystals yielded were solubilized by addition of a 5% solution of HCOOH in isopropanol. The MTT-formazan absorbance was read on a microprocessor controlled multiplate reader (Labexim LMR-1). The cell survival data were normalized as percentage of the untreated control (set as 100% viability) and were fitted to sigmoidal dose response curves and the corresponding IC<sub>50</sub> values (concentrations causing 50% suppression of cellular viability) were calculated.



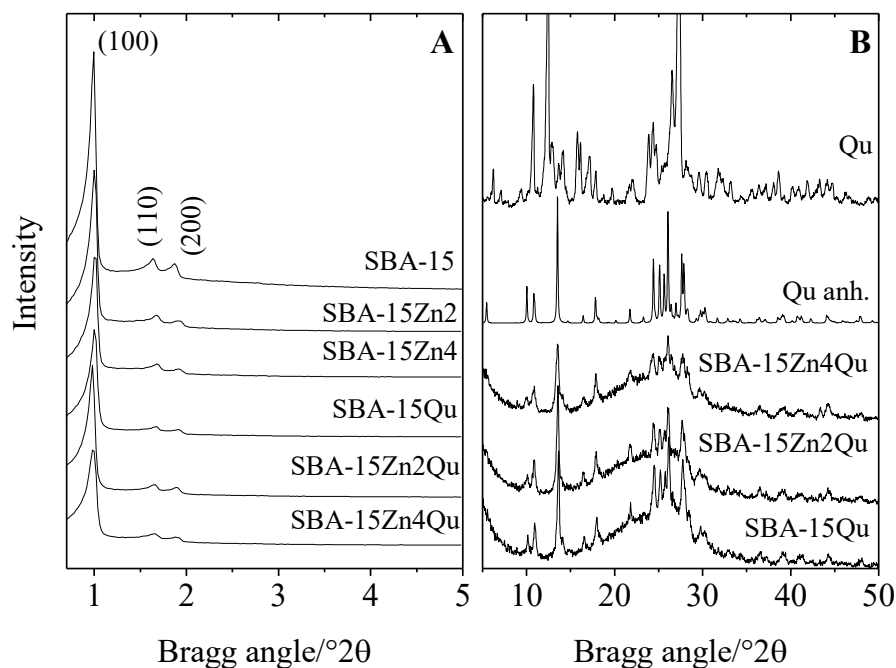


**Figure 1.** XRD patterns of quercetin loaded parent and Zn modified SBA-15 formulations compared to pure quercetin

### 3. Results and Discussion

#### 3.1. Material characterization

X-ray powder diffraction pattern of the parent SBA-15 sample at low 2 theta degree region confirms the formation of well-ordered 2 D hexagonal mesostructured. For the Zn-modified and quercetin loaded silica carriers somewhat decreased intensity and some broadened reflections are observed indicating some structural disorder or pore filling. XRD patterns at higher angles of quercetin loaded parent and Zn-modified samples (Fig.1) show the presence of crystalline quercetin. This is evidence that a part of quercetin can be found on the outer surface of the silica nanoparticles or in the voids among the particles.

Quercetin has three different hydrate forms, namely dihydrate (P-1), monohydrate (P2<sub>1</sub>/c) and anhydrous (P2<sub>1</sub>/a) form. The XRD patterns of the three forms were calculated by their single

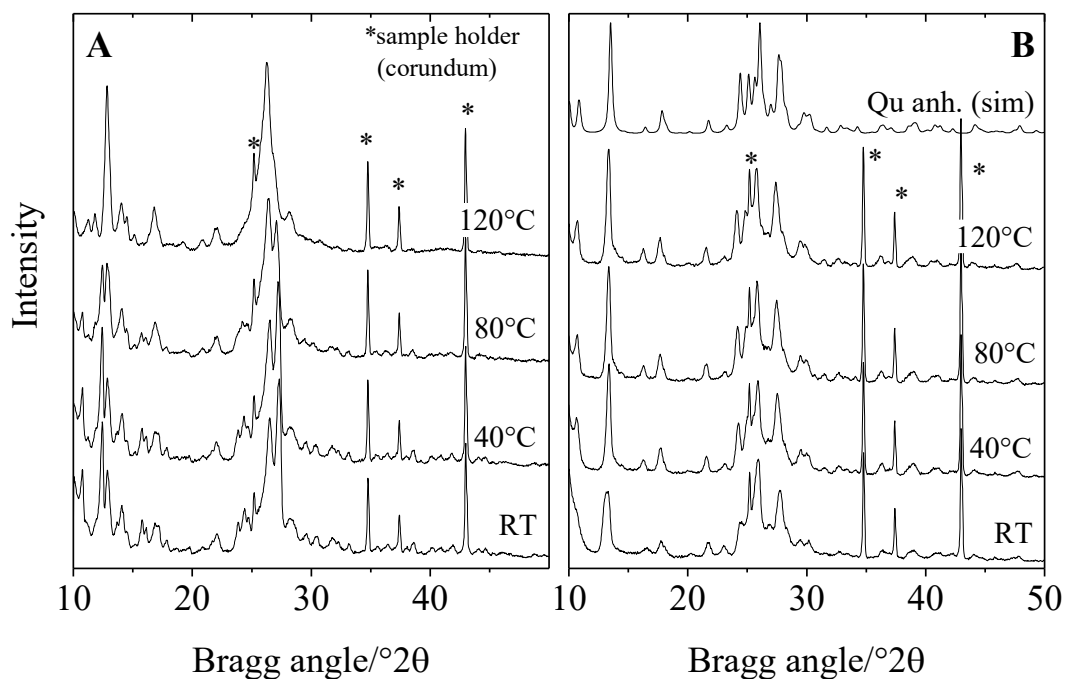


**Figure 2.** XRD patterns of the parent quercetin dihydrate (A) and the sample recrystallized in ethanol (B) recorded at RT, 40, 80, 120°C

crystal data deduced from Cambridge Structural Database, and from the publication of Filip et. al. [27].

Quercetin can be found in modified SBA-15 samples in its anhydrous form, independently whether it contains Zn or not, as experienced also by our former study with SBA-16 and MCM-41 support [32]. This is due to the recrystallization process of the drug in ethanol by the loading procedure. This was evidenced by recrystallizing the parent quercetin dihydrate in ethanol, and then in situ heat treating it at different temperatures up to 120°C (Fig. 2 B). It can be seen by the XRD patterns, that anhydrous form is readily crystallizes by the evaporation of ethanol at room temperature, and at elevated temperatures only the crystallinity is improved. However, direct heat treatment of the parent quercetin dihydrate results in the formation of another, not yet identified polymorph of anhydrite (Fig 2 A). Careful investigation of the parent quercetin dihydrate reveals that this material is a mixture of real dihydrate and the

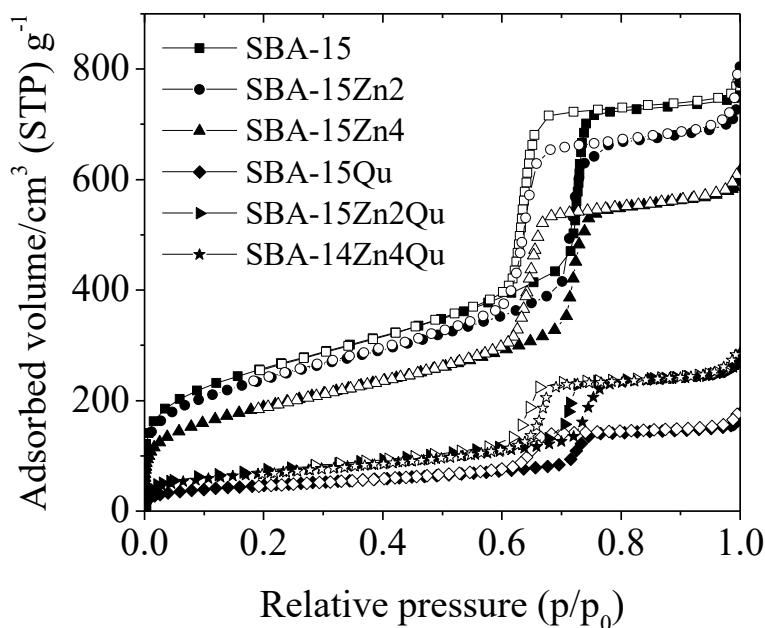


**Figure 3.** Nitrogen physisorption isotherms of the parent, Zn functionalized and quercetin-loaded SBA-15 samples.

unknown polymorph formed at 120°C heat treatment. This unknown polymorph is also recrystallizes to anhydrous form upon dissolving in ethanol or in methanol. We found as well, that this anhydrous form transforms to mono or dihydrate phase upon longer staying at ambient temperature and humidity. According to Srinivas et. al. water solubility of quercetin dihydrate and anhydrite is similar up to 80°C [33]. They have found that aqueous solubility of anhydrous quercetin varied from 0.00215 g/L at 25°C to 0.665 g/L at 140°C and that of quercetin dihydrate varied from 0.00263 g/L at 25°C to 1.49 g/L at 140°C. Thus, hydration state does not really influence the bioavailability of quercetin in dermal formulations, but can affect its other physical-chemical properties.

The nitrogen physisorption isotherms of the parent, and quercetin loaded siliceous and Zn-modified samples are presented in Fig. 3. Textural parameters are summarized in Table 1. The isotherms of the samples are of type IV with a H1 type hysteresis loop between 0.6-0.7 relative pressures, typical for SBA-15 structure. Significant decrease of the textural

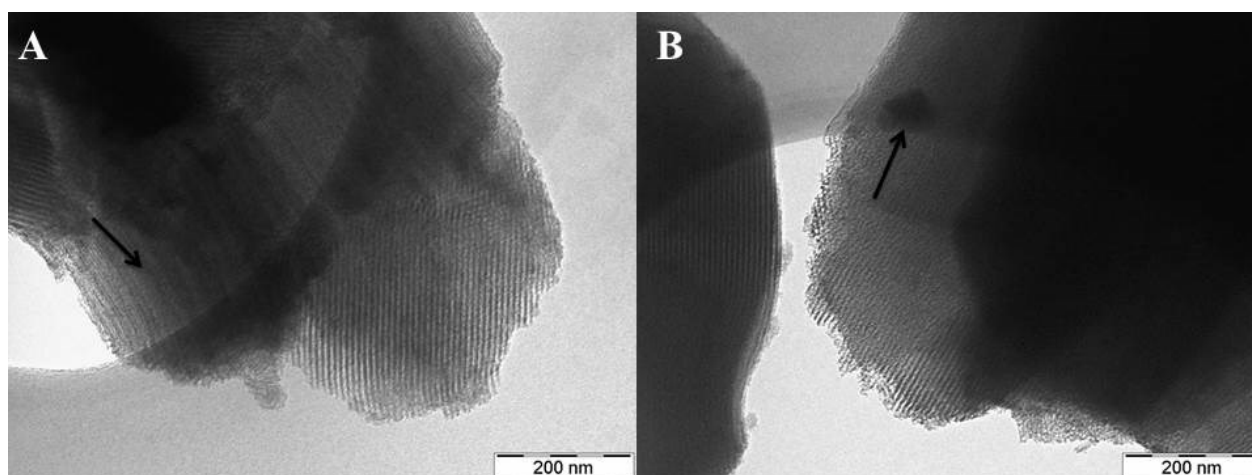


**Figure 4.** TEM images of 2 wt% (A), and 4 wt% Zn containing SBA-15 (B) samples.

parameters, such as surface area and total pore volume, of the quercetin loaded samples indicate pore filling by quercetin. Taking into account the mass of nitrogen adsorbing silica in the drug delivery system, we can calculate the ratio of filled pores by the drug. This amounts to ~65% for SBA-15Qu sample and about 25% for Zn containing samples. It seems that although Zn modification does not result in pore blocking of SBA-15 channels (Table 1) it hinders the penetration of quercetin into the channels, probably due to strong interaction of Zn with quercetin at the pore entrances. The pore filling by small ZnO nanoparticles (<5 nm) on SBA-15Zn2 sample as well as the presence of bigger Zn nanoparticles (around 20 nm) on SBA-15Zn4 are shown by TEM images (Fig.4 A and B), and this result is in good accordance with the N<sub>2</sub> physisorption data. The formation of rod shaped SBA-15 particles with sizes around 1-2  $\mu\text{m}$  was confirmed also by TEM investigation. The preservation of mesoporous structure after the quercetin deposition on both Zn-containing carriers was approved by TEM (not shown).

Information about the state of Zn in the silica matrix can be obtained by diffuse reflectance UV-Vis spectroscopic investigations. Spectra of Zn modified SBA-15 are shown in Fig. 5. On Zn modified samples no absorption band at around 350 nm can be observed, assigned to the

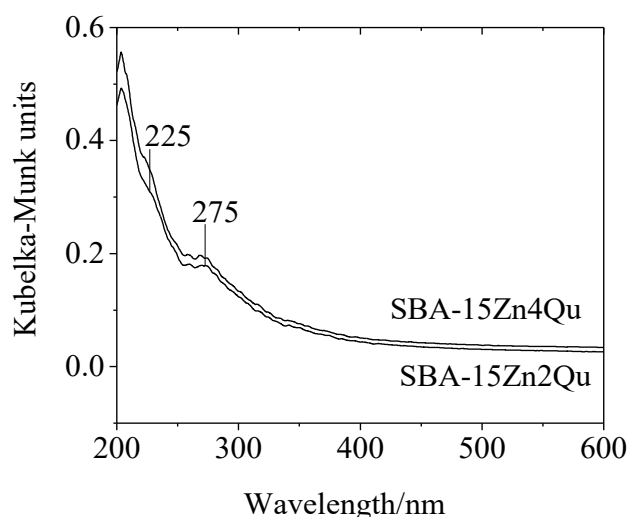


**Figure 5.** Diffuse reflectance UV-Vis spectra of Zn-containing SBA-15 samples

**Table 1** Textural properties of the studied samples and the quercetin content in the parent and Zn-functionalized samples.

Samples	BET (m <sup>2</sup> /g)	Pore volume (cm <sup>3</sup> /g)	PD <sup>a</sup> (nm)	Quercetin cont. (wt.%)
SBA-15	870	1.10	6.0	-
SBA-15Zn2	849	1.06	5.8	-
SBA-15Zn4	671	0.91	5.9	-
SBA-15Qu	163	0.23	5.8	41.8
SBA-15Zn2Qu	260	0.43	5.5	43.7
SBA-15Zn4Qu	233	0.38	6.0	45.5

<sup>a</sup> mean pore diameter calculated by the BJH model.

$O^{2-} \rightarrow Zn^{2+}$  ligand to metal charge transfer (LMCT) transition in bulk ZnO phase [34]. Nevertheless, absorption bands at 225 and 275 nm are registered. The bands appearing below 230 nm are associated with the charge transfer transitions of framework zinc species coordinated with lattice  $O^{2-}$  when metal atoms are incorporated into the silica framework, whereas the band around 280 nm can be considered as encapsulated zinc-oxide nanoparticles with size of 1-2 nm [34, 35]. It seems that Zn is distributed in SBA-15 in such a way that a part of it is incorporated into the silica matrix on the surface of pore walls, however there are also small ZnO nanoparticles inside the channels, or on the outer surface of the particles.

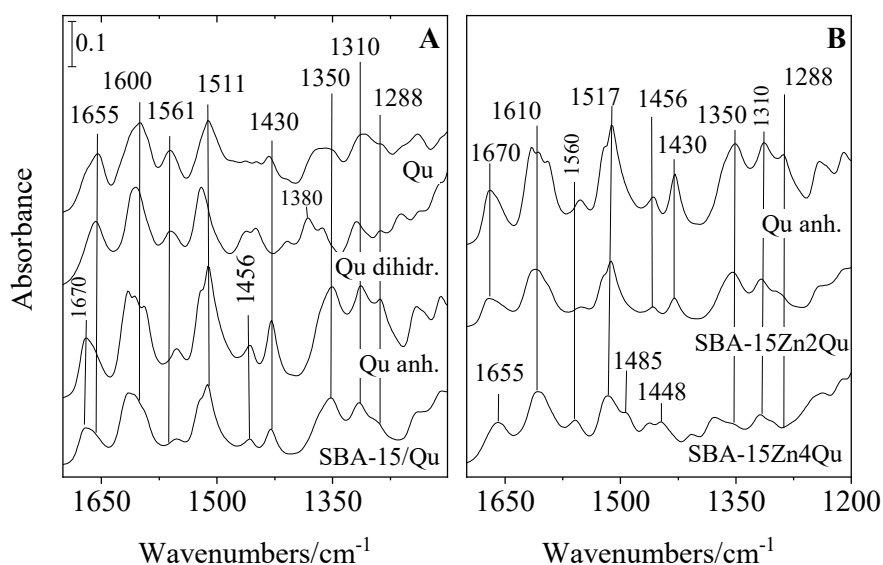


**Figure 6.** ATR FT-IR spectra of different quercetin hydrates and quercetin loaded parent (A) and Zn modified SBA-15 samples (B).

Compared to MCM-41 and SBA-16 structures [32], SBA-15 represents a transitional state. In our former study it was found that by Zn modification mainly ionic Zn species are formed in MCM-41. This can be due to the narrower pore size (~2.5 nm) and relatively higher amount of surface silanol groups of MCM-41. Because of the narrow pore entrances (~2.5 nm) in SBA-16, small ZnO particles are formed rather on the outer surface of the particles. In SBA-15 the pores are bigger (~6 nm) and there are enough silanol groups on the channel surface for Zn to react with, therefore both ionic Zn species and ZnO nanoparticles can be formed, either on the outer side or inside the channels. This different distribution of Zn species in the different types of silica structures strongly influences their interaction with quercetin as well. For clarification of the interaction between quercetin molecule, Zn and the mesoporous silica carrier the quercetin loaded samples were characterized by ATR FT-IR method (Fig. 6).

Parent quercetin shows characteristic IR bands of stretching vibrations of aryl ketonic carbonyl ( $\nu\text{C}=\text{O}$  at  $1670\text{--}1655\text{ cm}^{-1}$ ) and of aromatic ring  $\text{C}=\text{C}$  vibrations (at  $1610\text{--}1432\text{ cm}^{-1}$ ). The band at  $1350\text{ cm}^{-1}$  belongs to OH bending vibration of the phenols (likely on carbon atoms C3' and C4'), and the band around  $1309\text{ cm}^{-1}$  can be assigned as in-plane bending vibration of aromatic C-H [36-37]. Stretching vibration of C-O bond appears at around  $1290\text{ cm}^{-1}$ .

Since quercetin can be found in its anhydrous form on SBA-15 carrier, first we have to compare the spectra of different quercetin hydrates (Fig. 6 A). The spectra of the dihydrate and anhydrite forms show similarities, however, they can be clearly differentiated. In this respect, it can be observed that parent quercetin material is a mixture of anhydrite and dihydrate form, as evidenced also by XRD measurements. In dihydrate form the carbonyl  $\nu\text{C}=\text{O}$  vibration, due to the hydrogen bonds, can be found at  $1655\text{ cm}^{-1}$ , whereas this band is shifted to  $1670\text{ cm}^{-1}$  in the anhydrite form. In the aromatic ring  $\text{C}=\text{C}$  vibration region the bands in anhydrite form ( $1616, 1594, 1552, 1511, 1456$ , and  $1430\text{ cm}^{-1}$ ) seem to shift to upper wavelength ( $1606, 1558, 1519, 1463$  and  $1450\text{ cm}^{-1}$ ), too. In dihydrate form the  $\delta\text{C-OH}$  vibration of phenolic groups is shifted to  $1380\text{ cm}^{-1}$  compared to that of in anhydrous quercetin at  $1350\text{ cm}^{-1}$ . Also the vibrations of aromatic  $\delta\text{C-H}$  ( $1310\text{ cm}^{-1}$ ) and  $\nu\text{C-O}$  ( $1288\text{ cm}^{-1}$ ) are more intensive in anhydrite form.

Observing the spectrum of the SBA-15Qu sample, it rather resembles anhydrous quercetin more than the parent one, which is in accordance with XRD investigations. However, the intensity decrease of the  $1456, 1430$  and  $1288\text{ cm}^{-1}$  bands supports that physisorbed quercetin interacts with the silanol groups via aromatic rings rather than by phenolic groups.

FT-IR spectrum of SBA-15 sample modified with 2% of Zn and loaded with quercetin is quite similar to that of siliceous SBA-15 (Fig 6 B). However, for the 4 wt.% Zn containing sample some changes in the spectrum can be witnessed. The band at  $1456\text{ cm}^{-1}$  related to aromatic

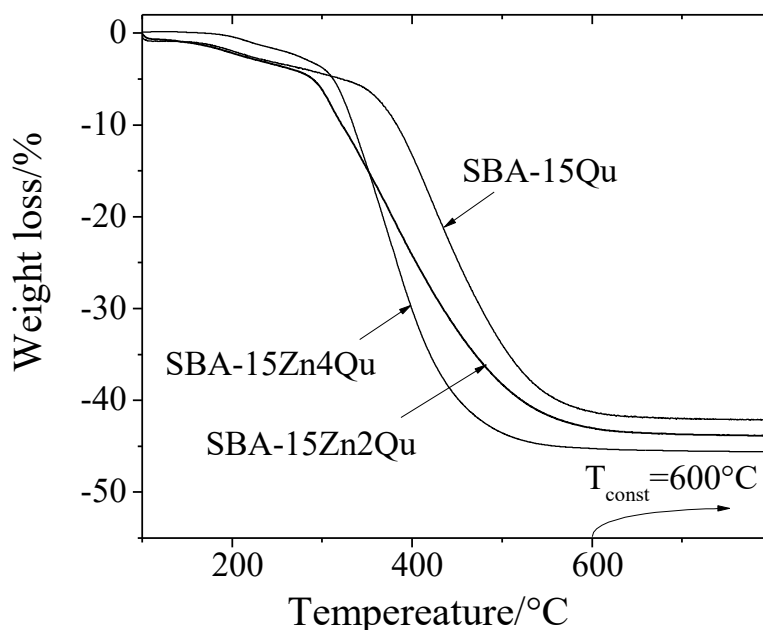


**Figure 7.** TG curves of quercetin loaded parent and Zn modified SBA-15 silica carriers.

C=C vibrations is split (into 1462 and 1448  $\text{cm}^{-1}$ , respectively) The band at 1430  $\text{cm}^{-1}$  (related to C-H deformation of aromatic A-ring) and that of  $\nu\text{C-O}$  vibration at 1288  $\text{cm}^{-1}$  also diminished. The main spectral change, however, is the disappearance of the broad, medium strong band belonging to OH bending ( $\delta\text{OH}$ ) of phenols at 1350  $\text{cm}^{-1}$ . All these changes reveal that mainly the aromatic ring (B-ring) of quercetin is affected by the interaction with the silica carrier. Since the C ring is fixed, probably the conformation of the quercetin molecule also changes (rotation of B-ring along the C-C connecting bond). Taking into consideration all the above spectral changes, it seems that the dominant interaction between Zn and quercetin occurs through the  $-\text{OH}$  groups of aromatic B-ring, in contrast to 4% Zn modified SBA-16, where the formation of Zn-quercetin complex involves the  $\text{C=O}$  group and the  $-\text{OH}$  groups of C-ring or A-ring [32].

### 3.2. Quercetin loading and in vitro release

Incipient wetness impregnation method was used for quercetin loading into the pores of SBA-15 and ZnSBA-15 silica carriers. The amount of quercetin in the prepared samples was



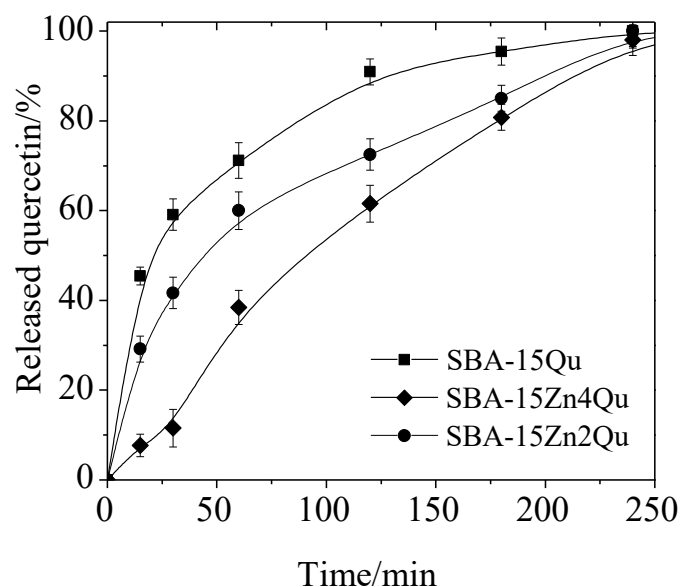


**Figure 8.** *In-vitro* release profiles of quercetin loaded parent and zinc modified SBA-15 samples at pH=5.5.

investigated by thermogravimetric method (Table 1). TG data (Fig. 7) show high loading of quercetin on all samples, it amounts more than 40 %. The similar quercetin loading for Zn-modified samples (43.7 % for SBA-15Zn2Qu and 45.5 % for SBA-15Zn2Qu) and the initial SBA-15 silica (41.6 %) is an indication that textural parameters are not significantly changed after the Zn modification (see Table 1).

*In vitro* release study of quercetin (Fig. 8) was conducted in phosphate buffer at pH=5.5, relevant to the physiological pH of the skin. The parent particles are characterized with initial burst effect, as almost 60 % of the drug is released within the first 30 min. In contrast to the parent silica, Zn modified samples showed slower quercetin release with no initial burst, which is more prominent for SBA-15Zn4 counterparts. However, the complete quercetin release was observed within 4 h for all samples. These differences in release profiles of Zn modified samples could be attributed to the formation of Zn-quercetin complexes, which are temporarily immobilized in the silica structure. The formation of water soluble Zn-quercetin

complexes is also supported by the fact that under the same experimental conditions hardly any Zn release is observed from SBA-15Zn2 and SBA-15Zn4 samples. After quercetin loading Zn release increased sharply (Table 1) to 65.5 wt.% for SBA-15Zn4Qu and to 100 wt.% for SBA-15Zn2Qu. This effect can also be associated with the formation of Zn-quercetin complex, making the metal content of the silica carrier soluble.

### ***3.3. Cytotoxicity assessment***

The lack of toxicity is an important requirement for all materials used in preparation of drug delivery systems. The cytotoxicity potential of mesoporous carriers was determined in two human cell lines with different cell types and origin, namely non-malignant HEK-293 and malignant HUT-78. The two cell lines were chosen in order to discriminate between the growth inhibitory potential of tested systems and free drug against non-tumorigenic and malignant cell lines. HEK-293 cells represent non-cancerous epithelial cells, whereas HUT-78 is a suitable model for cutaneous T-cell lymphoma (CTCL). A characteristic feature of CTCL is the constitutive over-activity of JAK-3 kinase, which is selectively inhibited by quercetin, making this polyphenol a potential targeted drug for this condition [38].

The growth inhibitory concentration-response curves are presented in Fig. 9 and the corresponding equieffective  $IC_{50}$  values are summarized in Table 2. The non-loaded silica particles failed to induce any significant decrease in cell viability of non-malignant HEK-293 cell line even at the highest dose of 1 mg/ml (not shown). The cytotoxicity of quercetin loaded mesoporous nanoparticles was determined on the same cell lines as empty NPs and compared with the effect on cell proliferation of free drug (Fig.8 A and B). As evident from the graphs quercetin and its SBA-15 and SBA-15Zn2 formulations did not show inhibitory effect on cell proliferation of non-malignant HEK-293 cells. Quercetin loaded SBA-15Zn4 causes eradication of app. 49 % of the treated cells, but even at the highest tested concentration  $IC_{50}$  values were not reached. In contrast, in malignant HUT-78 cells all tested formulations

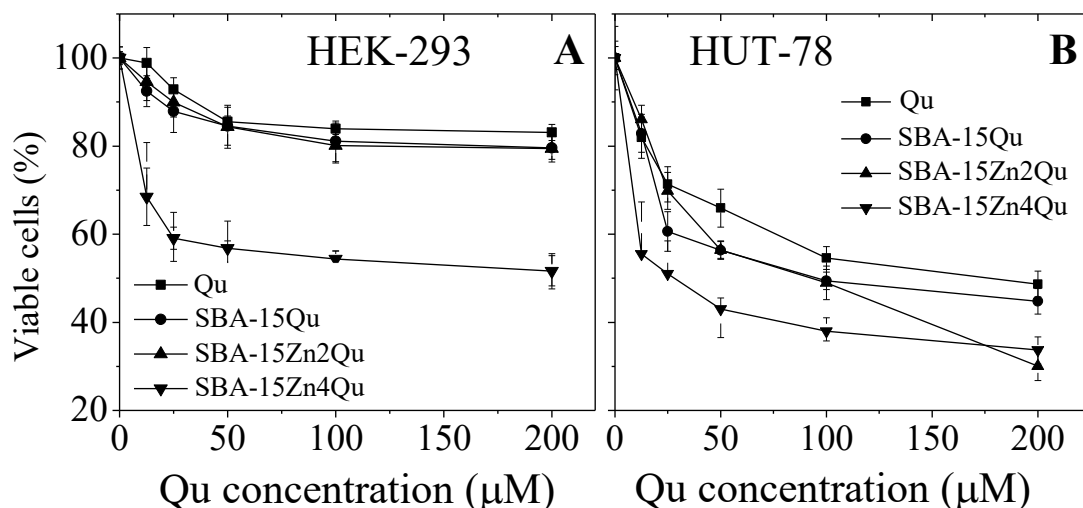


**Figure 9.** The concentration-response curves determined by the MTT-dye reduction assay after 72 hours continuous exposure. Each data point represents the arithmetic mean  $\pm$  SD of 8 separate experiments.

**Table 2** Equieffective concentrations of tested quercetin formulations, vs. the free drug.

Cell line	IC <sub>50</sub> (μM)			
	Quercetin	SBA-15Qu	SBA-15Zn2Qu	SBA-15Zn4Qu
HEK-293	n.d.	n.d.	n.d.	n.d.
HUT-78	174.8	95.14	91.3	26.5

exerted clear concentration dependent cytotoxic effects. These findings show that the tested quercetin loaded SBA-15 and SBA-15Zn2 formulations are characterized with high selectivity against malignant cells and are non-harmful for normal cells. In addition to their selectivity quercetin loaded mesoporous silica materials were superior in terms of cytotoxic activity as compared to the free quercetin compound. The concentration-response curves were shifted to the lower concentrations and respectively the IC<sub>50</sub> values were app. two folds lower as compared to the effects of quercetin, applied as an ethanol solution. This effect was more

pronounced in Zn-modified quercetin loaded particles, causing more than 70 % eradication of viable cells at the highest concentration 200  $\mu$ M.

#### **4. Conclusions**

Mesoporous SBA-15 silica was modified with different amounts of Zn (2 or 4 wt.%) by post-synthesis method. Quercetin was loaded by incipient wetness impregnation method with ethanol on the initial and Zn-modified SBA-15 samples by 1:1 ratio. By this loading method anhydrous quercetin was formed on the silica carrier. It was found that hydration forms of quercetin can be differentiated by XRD and by FT-IR spectroscopic methods. Thus, by evaluating the interaction of the drug with the silica carrier the changes due to its hydration state always have to be taken into account. It was shown that zinc is incorporated into the silica structure and ionic Zn species, as well as oxide nanoparticles encapsulated into the channels, or on the outer surface of silica particles are formed. Formation of Zn-quercetin complex was evidenced on zinc modified SBA-15 silica by FT-IR spectroscopy. High quercetin loading capacity (over 40 wt. %) was registered on the parent and Zn-containing SBA-15 samples. The *in-vitro* release process at pH=5.5 showed slower quercetin release from Zn-modified SBA-15 samples compared to the parent one. High quercetin loading and controlled release indicate that the obtained delivery systems are promising for dermal application. Additionally, the comparative cytotoxic experiments show that quercetin encapsulated in Zn-modified silica carrier (2 wt.% Zn) proved to exert superior antineoplastic potential against HUT-29 cells compared to free drug. Thus, it can be concluded that Zn-modified SBA-15 silica particles are promising carriers for dermal delivery of quercetin.

**Acknowledgements** Financial support from the Bulgarian-Hungarian Inter-Academic Exchange Agreement is greatly acknowledged. I. Trendafilova thanks the ДФНП-

191/14.05.2016 project for young scientists support funded by the Bulgarian Academy of Sciences.

## ***References***

- [1] I. Slowing, B. Trewyn, S. Giri, V. Lin, Mesoporous Silica Nanoparticles for Drug Delivery and Biosensing Applications, *Adv. Funct. Mater.* 17-8 (2007) 1225–1236.
- [2] S. Wang, Ordered mesoporous materials for drug delivery, *Microporous Mesoporous Mater.* 117 (2009) 1–9.
- [3] I. Slowing, J. Vivero-Escoto, C-W. Wu, V. Lin, Mesoporous silica nanoparticles as controlled release drug delivery and gene transfection carriers, *Adv. Drug Deliv. Rev.* 60 (2008) 1278–1288.
- [4] G. Owens, R. Singh, F. Foroutan, M. Alqaysi, Ch-M. Han, Ch. Mahapatra, H-W. Kim, Sol–gel based materials for biomedical applications, *Prog. Mater. Sci.* 77 (2016) 1–79.
- [5] M. Martínez-Carmona, M. Colilla, M. Ruiz-Gonzalez, J. Gonzalez-Calbet, M. Vallet-Regí, High resolution transmission electron microscopy: A key tool to understand drug release from mesoporous matrices, *Microporous Mesoporous Mater.* 225 (2016) 399-410.
- [6] T. Chen, W. Wu, H. Xiao, Y. Chen, M. Chen, J. Li, Intelligent Drug Delivery System Based on Mesoporous Silica Nanoparticles Coated with an Ultra-pH-Sensitive Gatekeeper and Poly(ethylene glycol), *ACS Macro Letters* 5-1 (2016) 55-58.
- [7] W. Wu, Ch. Ye, H. Xiao, X. Sun, W. Qu, X. Li, M. Chen, J. Li, Hierarchical mesoporous silica nanoparticles for tailorable drug release, *Inter. J. Pharm.* 511-1 (2016) 65-72.
- [8] I. Erlund, Review of the flavonoid quercetin, hesperetin, and naringenin. Dietary sources, bioactivities, bioavailability, and epidemiology, *Nutr. Res.* 24-10 (2004) 851-874.
- [9] J. Formica, W. Regelson, Review of the biology of quercetin and related bioflavonoids, *Food Chem. Toxicol.* 33 (1995) 1061–1080.

- [10] G.R. Beecher, B.A. Warden, H. Merken, Analysis of teapolyphenols, *Proc. Soc. Exp. Biol. Med.* 220 (1999) 267–270.
- [11] J. Kuhnau, The flavonoids. A class of semi-essential food components: their role in human nutrition, *World Rev. Nutr. Diet.* 24 (1976) 117-191.
- [12] W. Bors, C. Michel, M. Saran, Flavonoid antioxidants – rate constants for reactions with oxygen radicals, *Oxyg. Radic. Biol. Syst. D* 234 (1994) 420–429.
- [13] E.L. Da Silva, M.K. Piskula, N. Yamamoto, J.H. Moon, J. Terao, Quercetin metabolites inhibit copper ion-induced lipid peroxidation in rat plasma, *FEBS Lett.* 430 (1998) 405–408.
- [14] E. Vulcain, P. Goupy, C. Caris-Veyrat, O. Dangles, Inhibition of the metmyoglobin-induced peroxidation of linoleic acid by dietary antioxidants: action in the aqueous vs. lipid phase, *Free Radic. Res.* 39 (2005) 547–563.
- [15] M. Y. Moridani, J. Pourahmad, H. Bui, A. Siraki, P. J. O'Brien, Dietary Flavonoid Iron Complexes as Cytoprotective Superoxide Radical Scavengers, *Free Rad. Biol. & Med.* 34-2 (2003) 243–253.
- [16] J.-H. Yang, T.-C. Hsia, H.-M. Kuo, et al., Inhibition of lung cancer cell growth by quercetin glucuronides via G 2/M arrest and induction of apoptosis, *Drug Metab. Dispos.* 34-2 (2006) 296–304.
- [17] D.X. Hou, T. Kumamoto, Flavonoids as protein kinase inhibitors for cancer chemoprevention: direct binding and molecular modeling, *Antioxid. Redox. Signal.* 13 (2010) 691-719.
- [18] N.G. Cornejo, T.J. Boggon, T. Mercher, JAK3: a two-faced player in hematological disorders, *Int. J. Biochem. Cell. Biol.* 41(2009) 2376-2379.
- [19] A. P. Landi-Librandi, T. N. Chrysostomo, A. E. C. S. Azzolini, C.M. Marzocchi-Machado, C.A. de Oliveira, Y. M. Lucisano-Valim, Study of quercetin-loaded liposomes

- as potential drug carriers: In vitro evaluation of human complement activation, *J. Lipos. Res.* 22 (2012) 89–99.
- [20] A. Kumari, S.K. Yadav, Y.B. Pakade, B. Singh, S.C. Yadav, Development of biodegradable nanoparticles for delivery of quercetin, *Colloids Surf., B* 80 (2010) 184–192.
- [21] R. Fang, H. Jing, Z. Chai, G. Zhao, S. Stoll, F. Ren, F. Liu, X. Leng, Design and characterization of protein-quercetin bioactive nanoparticles, *J. Nanobiotechnol.* 9 (2011) 19.
- [22] Ch. Wang, B. Li, H. Li, Zn(II) chelating with peptides found in sesame protein hydrolysates: Identification of the binding sites of complexes, *Food Chem.* 165 (2014) 594–602.
- [23] J. Tan, B. Wang, L. Zhu, DNA binding, cytotoxicity, apoptotic inducing activity, and molecular modeling study of quercetin zinc(II) complex, *Bioorg. Med. Chem.* 17 (2009) 614–620.
- [24] J. P. Cornard, J. C. Merlin, Spectroscopic and structural study of complexes of quercetin with Al(III). *J. Inorg. Biochem.* 92 (2002) 19–27.
- [25] A. Ahmedova, K. Paradowska, I. Wawer,  $^1\text{H}$ ,  $^{13}\text{C}$  MAS NMR and DFT GIAO study of quercetin and its complex with Al(III) in solid state, *Inorg. J. Biochem.* 110 (2012) 27–35.
- [26] D. Zhao, Q. Huo, J. Feng, B.F. Chmelka, G.D. Stucky, Nonionic Triblock and Star Diblock Copolymer and Oligomeric Surfactant Syntheses of Highly Ordered, Hydrothermally Stable, Mesoporous Silica Structures, *J. Am. Chem. Soc.* 120-24 (1998) 6024–6036.

- [27] X. Filip, I-G. Grosu, M. Micla, C. Filip, NMR crystallography methods to probe complex hydrogen bonding networks: application to structure elucidation of anhydrous quercetin, *Cryst. Eng. Comm.*, 15 (2013) 4131-4142.
- [28] A. Szegedi, M. Popova, I. Goshev, Effect of amine functionalization of spherical MCM-41 and SBA-15 on controlled drug release, *J. Solid State Chem.* 184 (2011) 1201–1207.
- [29] A. Szegedi, M. Popova, K. Yoncheva, J. Makk, J. Mihály, P. Shestakova, Silver- and sulfadiazine-loaded nanostructured silica materials as potential replacement of silver sulfadiazine, *J. Mater. Chem. B* 2 (2014) 6283.
- [30] T. Mosmann, Rapid colorimetric assay for cellular growth and survival: application to proliferation and cytotoxicity assays, *J. Immunol. Methods* 65 (1983) 55-63.
- [31] S.M. Konstantinov H. Eibl, M.R. Berger, BCR-ABL influences the antileukaemic efficacy of alkylphosphocholines, *Br. J. Haematol.* 107 (1999) 365-380.
- [32] M. Popova, I. Trendafilova, Á. Szegedi, J. Mihály, P. Németh, S.G. Marinova, H.A Aleksandrov, G.N. Vayssilov, Experimental and theoretical study of quercetin complexes formed on pure silica and Zn-modified mesoporous MCM-41 and SBA-16 materials, *Micropor. Mesopor. Mater.* 228 (2016) 256-265.
- [33] K. Srinivas, J.W. King, L.R. Howard, J.K. Monrad, Solubility and solution thermodynamic properties of quercetin and quercetin dihydrate in subcritical water, *Journal of Food Engineering* 100 (2010) 208–218.
- [34] L. Wang, Sh. Sang, Sh. Meng, Y. Zhang, Y. Qi, Zh. Liu, Direct synthesis of Zn-ZSM-5 with novel morphology, *Mater. Lett.* 61-8,9 (2007) 1675-1678.
- [35] S. G. Hur, T.W. Kim, S.J. Hwang, S.H. Hwang, J.H. Yang, J.H. Choy, Heterostructured nanohybrid of zinc oxide-montmorillonite clay, *J. Phys. Chem.* 110-4 (2006) 1599-604.
- [36] M. Heneczowski, M. Kopacz, D. Nowak, A. Kuzniar, Infrared spectrum analysis of some flavonoids, *Acta. Pol. Pharm.* 58 (2001) 415-20.



- [37] M. Catauro, F. Papale, F. Bollino, S. Piccolella, S. Marciano, P. Nocera, S. Pacifico, Silica/quercetin sol–gel hybrids as antioxidant dental implant materials, *Sci. Technol. Adv. Mater.* 16 (2015) 035001 (11pp).
- [38] R. Boly, T. Gras, T. Lamkami, P. Guissou, D. Serateyn, R. Kiss, J. Dubois, Quercetin inhibits a large panel of kinases implicated in cancer cell biology, *Int. J. Oncol.* 38 (2011) 833-842.